AD-A085 087 LOS ALAMOS SCIENTIFIC LAB NM F/G 18/3
STUDIES OF LONG-TERM ECOLOGICAL EFFECTS OF EXPOSURE TO URANIUM --ETC(U)
MAY 80 G C WHITE, J C SIMPSON, K V BOSTICK
UNCLASSIFIED LA-8221 AFATL-TR-79-101 NL

1 OF 1
AD A
085087

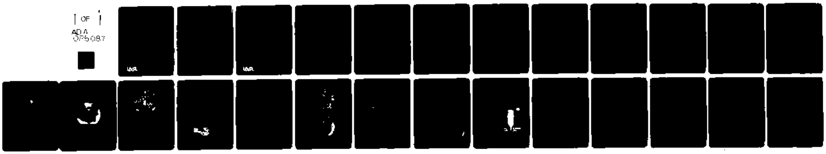

END
DATE FILMED
7-80
DTIC

LA-8221

AFATL-TR-79-101

LEVEL II

Studies of Long-Term Ecological Effects of Exposure to Uranium V

ADA085087

DDC FILE COPY

University of California

LOS ALAMOS SCIENTIFIC LABORATORY

Post Office Box 1663 Los Alamos, New Mexico 87545

80 6 2 055

An Affirmative Action/Equal Opportunity Employer

This is a completion report of Project Order ATL-9-138 to Reimbursable Activities Branch, US Department of Energy, Albuquerque, New Mexico, from the US Air Force Armament Laboratory, Eglin AFB, Florida.

Edited by Elaine Stanlick
Photocomposition by Christine West

UNITED STATES
DEPARTMENT OF ENERGY
CONTRACT W-7405-ENG. 36

LA-8221
AFATL-TR-79-101

UC-11
Issued: May 1980

Studies of Long-Term Ecological Effects of Exposure to Uranium V.

Gary C. White
Jeanne C. Simpson*
Kenneth V. Bostick

Final rept.

*Battelle Pacific Northwest Laboratories, Energy Systems Department, P.O. Box 999, Richland, WA 99352.

SECURITY CLASSIFICATION OF THIS PAGE (When Data Entered)

REPORT DOCUMENTATION PAGE

READ INSTRUCTIONS BEFORE COMPLETING FORM

1. REPORT NUMBER: AFATL-TR-79-101	2. GOVT ACCESSION NO.: AD-A085 087
3. RECIPIENT'S CATALOG NUMBER	
4. TITLE (and Subtitle): Studies of Long-Term Ecological Effects of Exposure to Uranium V	5. TYPE OF REPORT & PERIOD COVERED: Final Report 1 Oct 78 - 30 Sep 79
	6. PERFORMING ORG. REPORT NUMBER: LA-8221
7. AUTHOR(s)	8. CONTRACT OR GRANT NUMBER(s): Project Order ATL-9-138
9. PERFORMING ORGANIZATION NAME AND ADDRESS	10. PROGRAM ELEMENT, PROJECT, TASK AREA & WORK UNIT NUMBERS: Program Element 62602F JON 06CD0102
11. CONTROLLING OFFICE NAME AND ADDRESS: AFATL/DLV Eglin AFB, FL 32542	12. REPORT DATE: May 1980
	13. NUMBER OF PAGES: 26
14. MONITORING AGENCY NAME & ADDRESS (if different from Controlling Office)	15. SECURITY CLASS. (of this report): Unclassified
	15a. DECLASSIFICATION/DOWNGRADING SCHEDULE

16. DISTRIBUTION STATEMENT (of this Report)

APPROVED FOR PUBLIC SALE. DISTRIBUTION UNLIMITED.

17. DISTRIBUTION STATEMENT (of the abstract entered in Block 20, if different from Report)

18. SUPPLEMENTARY NOTES

19. KEY WORDS (Continue on reverse side if necessary and identify by block number)

Uranium, Depleted Uranium, Uranium Analysis, Phoswich Portable Survey Instrument, Epithermal Neutron Activation, Statistical Analysis, Kriging, Bluepack

20. ABSTRACT (Continue on reverse side if necessary and identify by block number)

Research performed by the Los Alamos Scientific Laboratory for the Air Force Armament Laboratory, Eglin Air Force Base, Florida, is reported. A Statistical Technique known as kriging was used to analyze the uranium concentrations in surface soil at E-F Site (LASL). Kriging provided a much more realistic contour surface for U concentrations than either a polynomial trend analysis or contouring the original data. The major advantages of kriging are: 1) a measure of the uncertainity of the contoured surface is provided,

DD FORM 1 JAN 73 1473 EDITION OF 1 NOV 65 IS OBSOLETE

SECURITY CLASSIFICATION OF THIS PAGE (When Data Entered)

20.

and 2) the nonparametric nature of the method allows very irregular surfaces to be fitted. A function relating the counting efficiency for uranium of the phoswich portable survey instrument to ambient temperature (10°C-30°C) was developed. Counting efficiency is maximum at approximately 10°C and declines significantly for higher temperatures. Soil moisture and relative humidity were also considered, but did not affect the counting efficiency of the phoswich.

A

STUDIES OF LONG-TERM ECOLOGICAL

EFFECTS OF EXPOSURE TO URANIUM V

by

Gary C. White, Jeanne C. Simpson, and
Kenneth V. Bostick

ABSTRACT

Research performed by the Los Alamos Scientific Laboratory (LASL) for the Air Force Armament Laboratory, Eglin Air Force Base, Florida, is reported. A statistical technique called kriging was used to analyze the uranium concentrations in surface soil at E-F Site (LASL). Kriging provided a much more realistic contour surface for uranium concentrations than either a polynomial trend analysis or contouring the original data. The major advantages of kriging are that a measure of the uncertainty of the contoured surface is provided, and that the nonparametric nature of the method allows very irregular surfaces to be fitted. A function relating the uranium counting efficiency of the phoswich portable survey instrument to ambient temperature (10−30°C) was developed. Counting efficiency is maximum at approximately 10°C and declines significantly at higher sample temperatures. The counting efficiency of the phoswich was not affected by soil moisture or relative humidity.

I. INTRODUCTION

This report summarizes results from October 1, 1978—September 30, 1979, of research performed by the Los Alamos Scientific Laboratory (LASL) for the Air Force Armament Laboratory, Eglin Air Force Base (EAFB), Florida. Included are (1) an evaluation of kriging to estimate soil concentrations of uranium in the environment, (2) an evaluation of the counting efficiency of the phoswich portable survey instrument relative to changes in temperature, humidity, and soil moisture of the sample, and (3) comparison of phoswich counts to epithermal neutron activation analysis (IENA) from EAFB Test Area C-74L.

The general scope and objectives of this study and the site descriptions were presented in previous reports.[1-3] Objectives of the research efforts reported here were

- to evaluate the usefulness of kriging to estimate soil uranium concentrations, and
- to develop a counting efficiency curve for the phoswich portable survey instrument when used to measure soil uranium concentrations in the field.

This research has application in field situations where substantial amounts of uranium have been released to the environs and an inventory to discover the fate of the contaminant is required.

II. EVALUATION OF KRIGING FOR E-F SITE SOILS

A statistical technique called kriging was used to analyze the uranium concentrations in the surface soil at E-F Site (LASL). Kriging is a relatively new statistical approach to spatial estimation developed by the French and South Africans for use in geological studies. In this report, a brief and simplistic overview of kriging is given, and is a summary of information given by Doctor.[4]

Kriging is based on a relationship of the form $Z(\underline{x}) = m(\underline{x}) + u(\underline{x})$, where

$Z(\underline{x})$ is the observed value of the phenomenon at location $\underline{x}$,

$m(\underline{x})$ is the drift, a function that describes the deterministic component, and

$u(\underline{x})$ is a function that describes the relationship between the observations.

The term $u(\underline{x})$ is very important in kriging. For any two locations ($\underline{x}_1$ and $\underline{x}_2$) suppose that $u(\underline{x}_1)$ and $u(\underline{x}_2)$ are related and that the relationship can be described as a function of the intervening distances ($\underline{h}$). Kriging uses this structure to provide the "best" *estimate of $Z(\underline{x})$ at location $\underline{x}$ from the surrounding* data.

Kriging assumes that the first-order difference

$$Z(\underline{x} + \underline{h}) - Z(\underline{x})$$

forms a stationary process, which must hold only over the distance used to make an estimate and, thus is referred to as local stationarity.

Three equally important interlocking aspects of kriging are

- Range - the proximity of the data to the point of interest.
- Drift - the large-scale phenomenon. If the distance over which the data are drawn to make an estimate is larger than the distance over which the local stationarity holds, then there is a drift.
- Structure - the variogram or generalized covariance function. This provides information on the form of the relationship between two observations as a function of the intervening distance.

The theoretical variogram is (E is expectation operator)

$$\lambda(|h|) = \frac{1}{2} E[Z(\underline{x} + \underline{h}) - Z(\underline{x})]^2 \quad .$$

The sample variogram is (N is number of data points in $\underline{x}$)

$$C(|\underline{h}|) = \frac{1}{2N} \sum_{\underline{x}} [Z(\underline{x} + \underline{h}) - Z(\underline{x})]^2 \quad .$$

The variogram has many possible shapes. Figure 1A shows a relationship between observations that changes regularly over distance. The range over which the surrounding data give information about the point being estimated is h_0. Observations farther apart than h_0 are considered independent. The sill is a measurement of the basic variability between two unrelated observations. Figure 1B shows a linear variogram with a nugget effect, which is a combination of the discontinuity in the phenomenon,

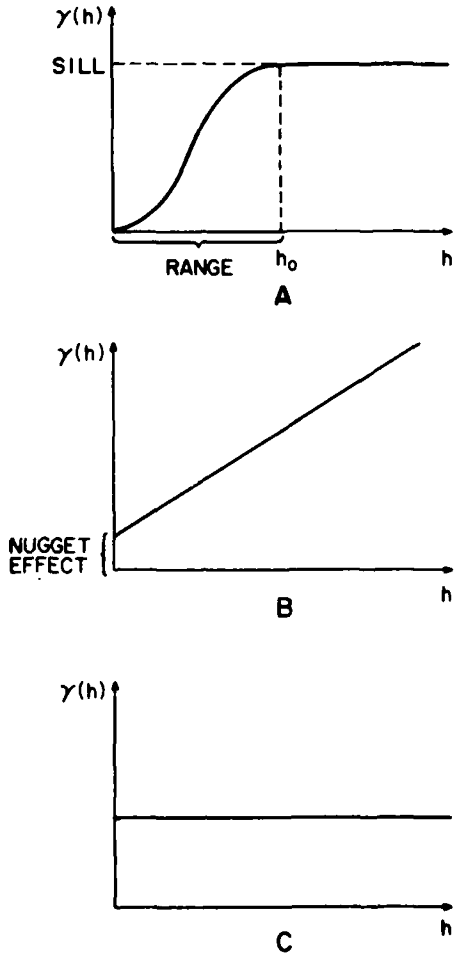

Fig. 1.
Examples of different types of variograms.

measurement error, and/or variability within the sample. The nugget effect can be part of any type of variogram. The linear variogram shows a phenomenon where the variability increases linearly with increasing distance between the two observations. In theory, this can continue forever, but in reality, there is a distance at which one observation provides no information about another observation. Figure 1C, a variogram of pure nugget effect, implies that there is no correlation structure to the phenomenon; that is, all the observations are independent.

One of the difficulties with the variogram is that it is legitimate only when the drift is constant; otherwise, the drift is included in the variogram and must be extracted from it. Fortunately, only the order of the drift (constant, linear, quadratic) must be known because the drift parameters cancel in the kriging equations.

One approach to the drift and structure identification problem is to make use of the algebraic property: higher order differencing filters out polynomials. Kriging uses this property, calling it generalized increments, to provide a locally stationary variable from one that has a drift. This is an n-dimensional analog of the Box-Jenkins approach to time series analysis. The advantage is that the covariance structure of the spatial variable can then be estimated without the effect of the drift. For example, a one-dimensional phenomenon $Z(x)$ has a linear drift; that is, $E[Z(x)] = a_0 + a_1x$.

The difference of the two first-order differences, where $x_2 - x_1 = x_1 - x_0$, has a zero expectation $E\{[Z(x_2) - Z(x_1)] - Z(x)_1 - Z(x_0)]\} = 0$, and the phenomenon represented by this second-order difference, $Z(x_2) - 2Z(x_1) + Z(x_0)$, is now stationary. The generalized covariance function is determined from this stationary phenomenon.

Information about the range, drift, and structure (variogram or generalized covariance function) is used to develop a set of linear equations that are solved to find the optimal weights to apply to the values observed at some other point. This kriging estimate has the statistical properties of being unbiased and minimum variance.

The kriging variance is a theoretical or model variance and not an empirical measure of lack of fit. The variance can be interpreted as how much the different realizations of the surface could vary with the same underlying drift and covariance structure.

The kriging analysis, done by the computer program BLUEPACK, allows a large amount of flexibility. Before analysis, BLUEPACK has many options for manipulating and viewing the data:

- listing,
- display,
- histogram,
- user-specified rejection of data points,
- user-specified data transformations, and,
- changes in the coordinate system.

BLUEPACK automatically identifies and tests the optimum drift and covariance function or the user may specify the model to be used. BLUEPACK can estimate values and standard deviations for

- isolated points,
- nodes of a complete or masked-off grid,
- averages over grid blocks,
- averages over an irregular territory,
- sections, and
- total inventory.

These results can be listed and contoured on a line printer or stored on magnetic tape for use by another plotting routine.

A polar coordinate sampling pattern was used to collect the data at E-F Site (Fig. 2). Core samples were taken at the intersections of radii that extended from the detonation point every 45 degrees and from concentric circles 10, 20, 30, 40, 50, 75, 100, 150, and 200 m from the detonation point. Of these 72 samples, 67 were available for analysis. Ten additional samples, taken at 0.5 m from some of the above intersections, were analyzed.

The core samples were 2.5-cm diam and from depths to 30 cm. The cores were cut into segments corresponding to depths from 0.0 to 2.5, 2.5 to 5.0, 5.0 to 10.0, 10.0 to 15.0, 15.0 to 20.0, and 20.0 to 30.0 cm. The segments were analyzed by a fluorometric technique to determine the micrograms of uranium per gram of soil. Kriging was used to analyze the data, shown in Table I, from the 0.0- to 2.5-cm segment.

Figure 3A is a histogram of the uranium concentrations listed in Table I. The data are obviously very skewed to the left. Therefore, before kriging, the data were transformed using the natural logarithm. Figure 3B, a histogram of the transformed data, now shows an approximately normal distribution

The sample variogram of the data shown in Fig. 4 gives the impression of a nugget effect and either a linear or parabolic curve. The nugget effect indicates

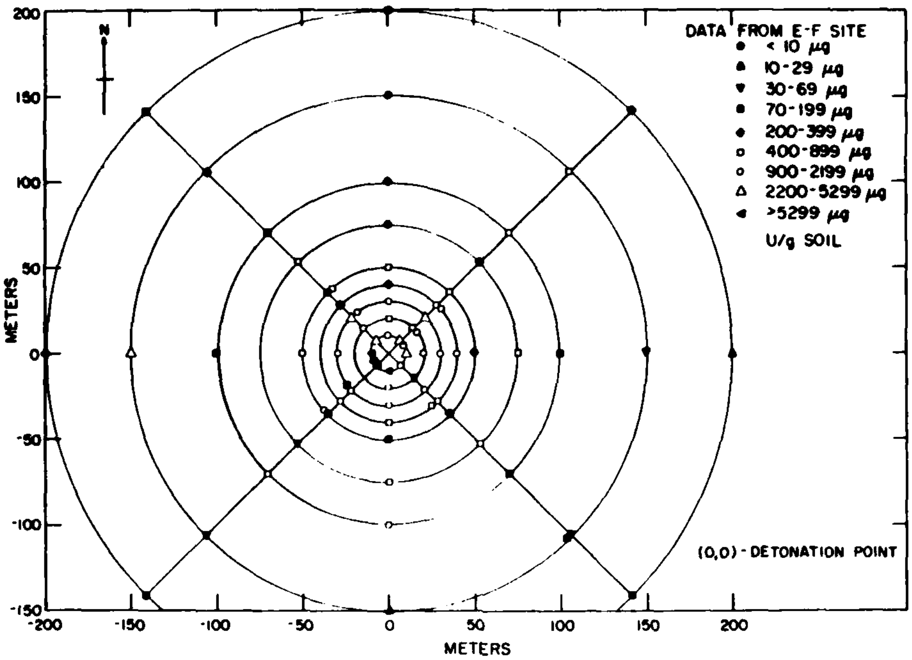

Fig. 2.
Polar coordinate sampling pattern used at E-F Site.

either a discontinuity in the phenomenon, measurement error, and/or within-sample variability. The somewhat parabolic character of the curve indicates a possible nonconstant drift.

BLUEPACK's automatic structure identification option was performed. It chose a linear drift and a generalized covariance function with nugget and linear components $K(|\underline{h}|) = 0.1176 - 0.08854\,|\underline{h}|$, which is consistent with the sample variogram.

The kriged contour map of the uranium concentrations, using this drift and covariance structure, is shown in Fig. 5. For comparison, the contour map of the same data reported by Hanson and Miera[2] is shown in Fig. 6. Although the maps are not identical, we will show later that when the kriging standard errors are considered, the contour map from Ref. 2 basically falls within the bounds of the expected realizations of the surface, given this underlying drift and covariance structure.

A contour map of the kriging standard errors (square root of the kriging variance) shown in Fig. 7 is an obvious reflection of our sampling pattern. Since the covariance function has a linear component, kriging uses the surrounding information (data) to make an estimate. The greater the distance that kriging must go to get this information, the greater the variability. The closer to the detonation point (where there is the greatest amount of data) the smaller the variability; the farther from the detonation point, the greater the variability becomes, especially in the areas between the radii.

Keep in mind that the variability discussed here is not a lack-of-fit variability, but the ways in which the realizations of the surface could vary, given the underlying drift and covariance structure. One way to look at the fit or lack of fit of the kriged surface is to compare it with a visual inspection of the surface. The kriged surface fits quite well, far better than that in Fig. 6.

The interpretation of the kriging estimates and their errors is complicated by the fact that the original data were transformed by natural logarithms before kriging. In the transformed space, kriging estimated the mean for a given point, and using normal theory approximation, the kriging standard errors can be used to set a confidence interval. When the kriging estimates are transformed back to the original space, the mean estimate becomes an estimate of the median, the standard errors become multiplicative instead of additive, and the confidence interval becomes asymmetrical. Thus, although the kriging standard errors in Fig. 7

TABLE I

URANIUM CONCENTRATIONS AT E-F SITE FROM REF. 2

Coordinates X (m)	Coordinates Y (m)	Concentration µg Total U per g Soil	Coordinates X (m)	Coordinates Y (m)	Concentration µg Total U per g soil
−200.00	0.00	390	0.00	−20.00	1400
−150.00	0.00	4900	0.00	−30.00	1100
−141.42	141.42	195	0.00	−40.00	862
−141.42	−141.42	9	0.00	−50.00	95
−106.07	106.07	292	0.00	−75.00	552
−106.07	−106.07	45	0.00	−100.00	2000
−100.00	0.00	93	0.00	−150.00	22
−70.71	70.71	94	7.07	7.07	2632
−70.71	−70.71	809	7.07	−7.07	995
−53.03	53.03	662	7.42	6.72	420
−53.03	−53.03	65	10.00	0.00	4750
−50.00	0.00	720	14.14	14.14	896
−35.70	−35.00	1100	14.14	−14.14	63
−35.36	35.36	105	14.49	13.79	1900
−35.36	−35.36	157	20.00	0.00	947
−35.00	35.70	417	21.21	21.21	3100
−30.00	0.00	1300	21.21	−21.21	940
−28.28	28.28	240	27.93	−28.63	525
−28.28	−28.28	658	28.28	28.28	1500
−21.56	−20.86	94	28.28	−28.28	725
−21.21	21.21	3900	28.63	27.93	887
−21.21	−21.21	482	30.00	0.00	1500
−20.86	21.56	1100	35.36	35.36	515
−14.14	14.14	2000	35.36	−35.36	360
−10.00	0.00	5700	40.00	0.00	902
−7.42	−6.72	7800	50.00	0.00	392
−7.07	7.07	2700	53.03	53.03	238
−7.07	−7.07	8600	53.03	−53.03	405
0.00	200.00	100	70.71	70.71	716
0.00	150.00	9	70.71	−70.71	135
0.00	100.00	225	75.00	0.00	539
0.00	75.00	3	100.00	0.00	90
0.00	50.00	805	105.72	−106.42	155
0.00	40.00	331	106.07	106.07	416
0.00	30.00	2100	106.07	−106.07	65
0.00	20.00	697	141.42	141.42	335
0.00	10.00	1100	141.42	−141.42	6
0.00	−10.00	11700	150.00	0.00	58
			200.00	0.00	16

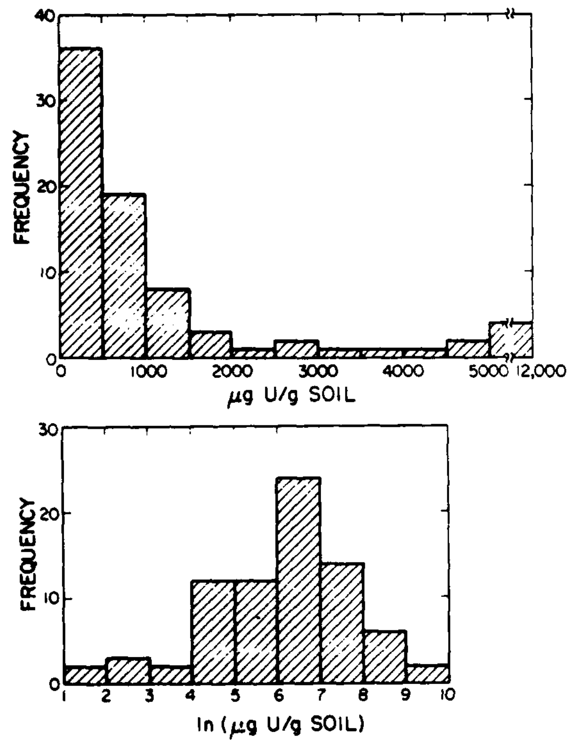

Fig. 3.
Histogram of uranium concentrations from E-F Site.

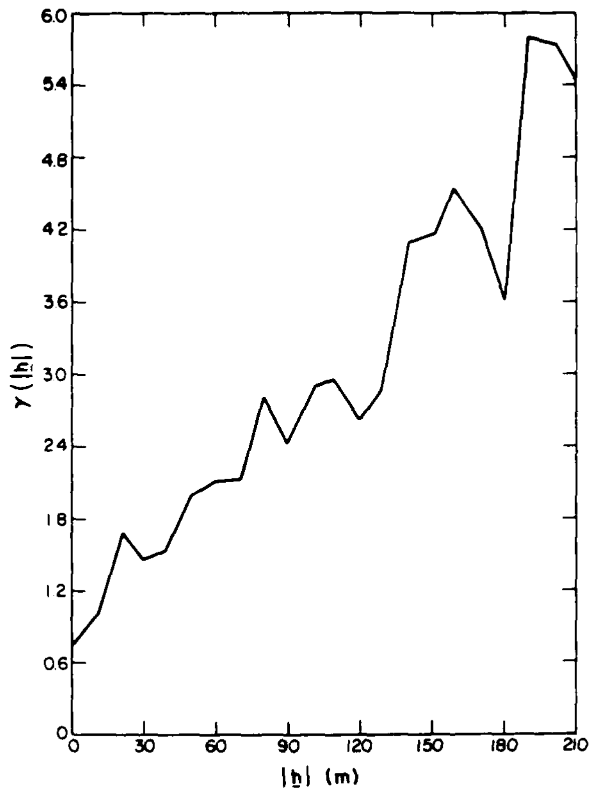

Fig. 4.
Sample variogram for uranium concentrations from E-F Site.

seem small compared to the kriging estimates in Fig. 5, when they are used multiplicatively to set confidence intervals on the kriging estimates, the intervals become quite large.

We are undecided as to the best way to demonstrate the variability in the kriged contour map, so we show three approaches to this problem.

We set confidence intervals about the kriging estimates in the transformed space, and then transformed the bounds back to the original space to make contour maps. Since the kriging standard errors were so large, we used only an ~68% confidence interval (plus or minus one standard error). Figures 8 and 9 are the contour maps of the upper and lower bounds of the kriged surface, and they show a large amount of variability.

We extended that approach by lengthening the contours of the confidence intervals, as shown in Fig. 10. Almost half the area being kriged had ~68% confidence intervals with lengths over 1000 µg, whereas Fig. 5 shows that much of this same area had estimates of less than 1000 µg. The large confidence intervals to the west of the detonation point are attributed to the abnormally high concentration of uranium (4900 µg) at (−150,0) compared with its two nearest points [390 µg at (−200,0) and 93 µg at (−100,0)]. This abnormally high concentration combined with the large distances over which kriging must go to get estimate information has caused this entire area to be quite variable. The large confidence intervals around the detonation point are a reflection of the multiplicative nature of the error; even though the kriging standard errors are small, the large estimates in this area lead to large confidence intervals.

We extended the first approach again by setting ~68% confidence bands on the isopleths. This is done by tracing a given isopleth from Figs. 8 and 9 onto a single page, thus creating a band within which the true isopleth lies with ~68% confidence

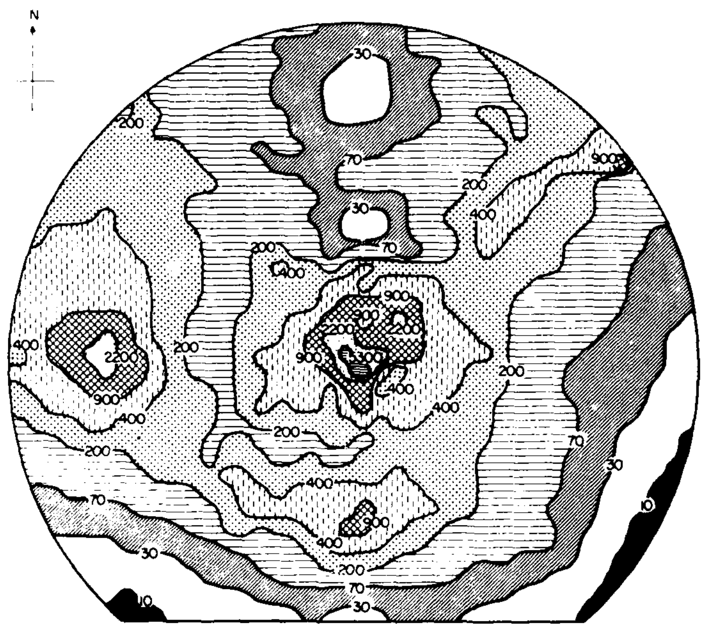

Fig. 5.
Kriged contour map of uranium concentrations (μg U/g soil) from E-F Site using BLUEPACK structure.

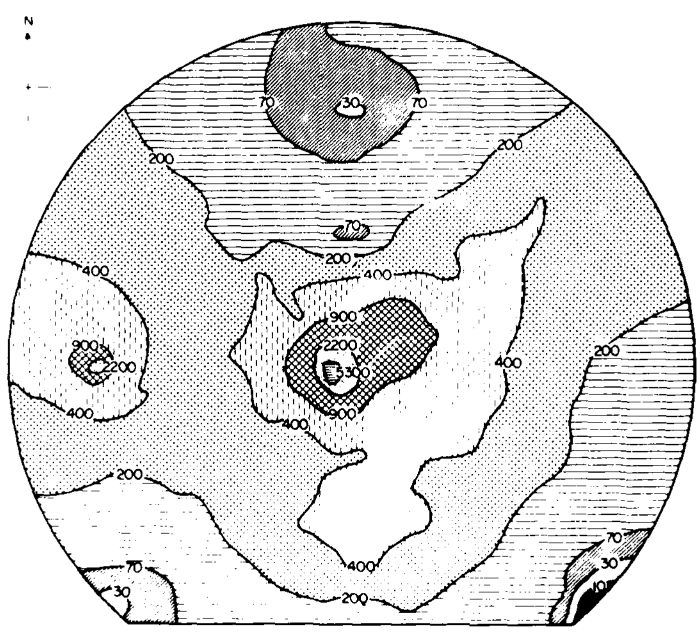

Fig. 6.
Contour map of data reported in Table I of uranium concentrations at E-F Site (from Hanson and Miera[2]).

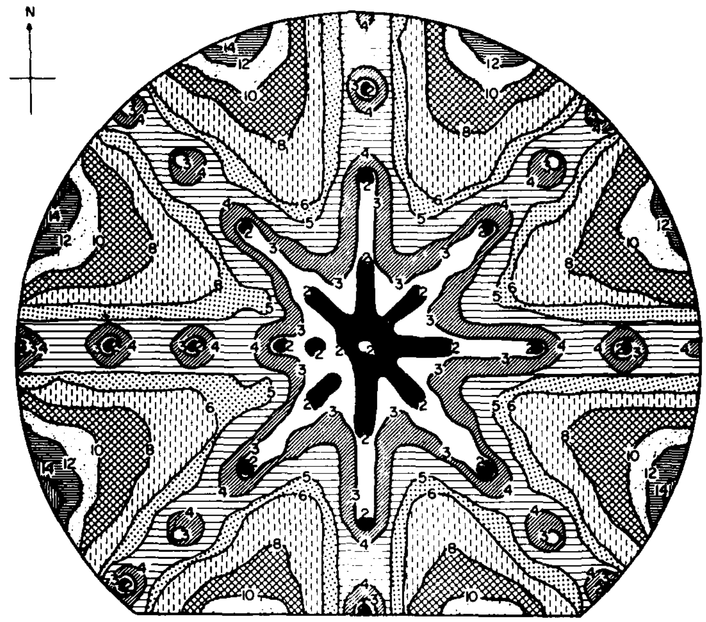

Fig. 7.
Contour map of kriging standard errors (μg U/g soil) (square root of kriging variance) in data from E-F Site.

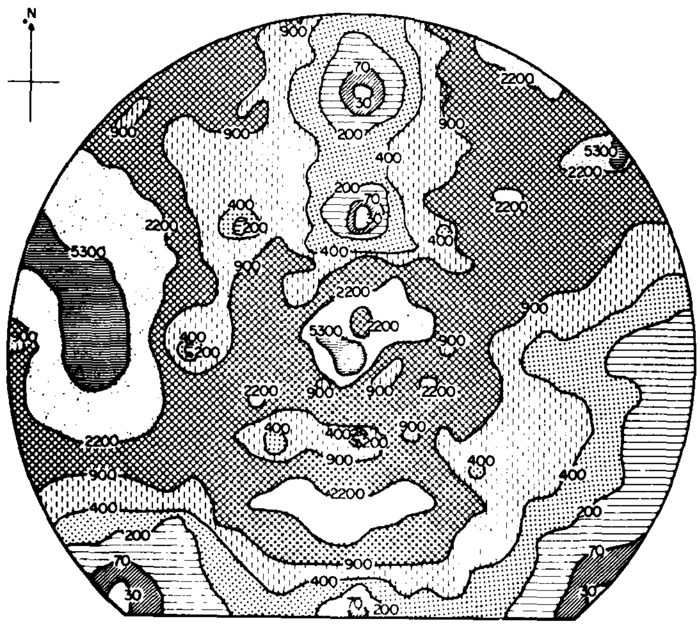

Fig. 8.
Contour map of the upper bound (μg U/g soil) of the kriged surface.

level. The areas with the diagonal stripes in Figs. 11-18 are the 68% confidence bands for the 5300- to 10-μg isopleths. The black lines on these figures show the actual kriged isopleths from Fig. 5. The larger isopleths (5300 and 2200 μg) and the smallest isopleth (10 μg) have comparatively small bands, and the rest have very large bands. In many cases, well over 50% of the area kriged is included in these bands. Essentially, the kriging variance states that the middle isopleths (30 to 900 μg) could be almost anywhere and still be "near" the true surface.

No matter which of the three approaches is used, there is a large amount of variation in the surface estimated by kriging. Figure 6 (data from Ref. 2) shows that, with few exceptions, the contours based on raw data fall within the ~68% confidence bounds of the kriged surface. We believe that this estimate of variability is one of the important features of kriging. Although the kriged surface "fits" the data well, it is apparent from the kriging variance that the true realization of this surface can vary substantially from the estimated surface.

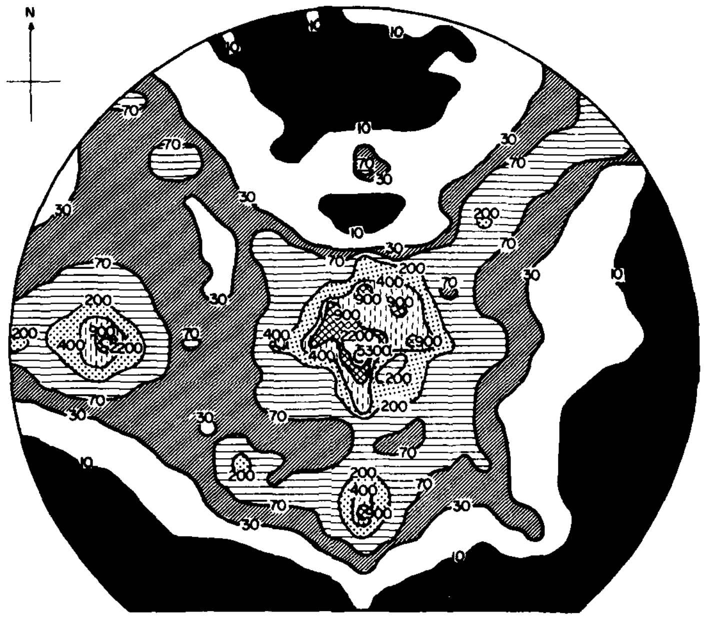

Fig. 9.
Contour map of the lower bound (μg U/g soil) of the kriged surface.

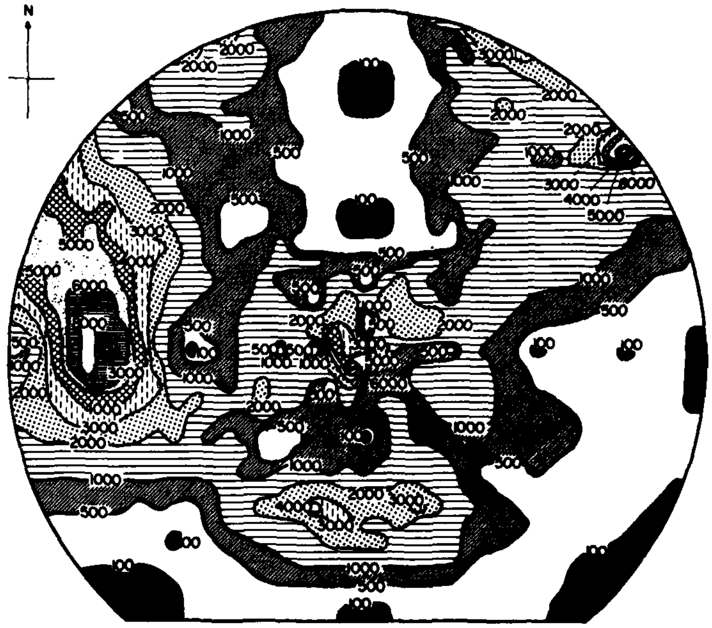

Fig. 10.
Contour map of the length of the 68% confidence intervals (μg U/g soil) of the kriged surface.

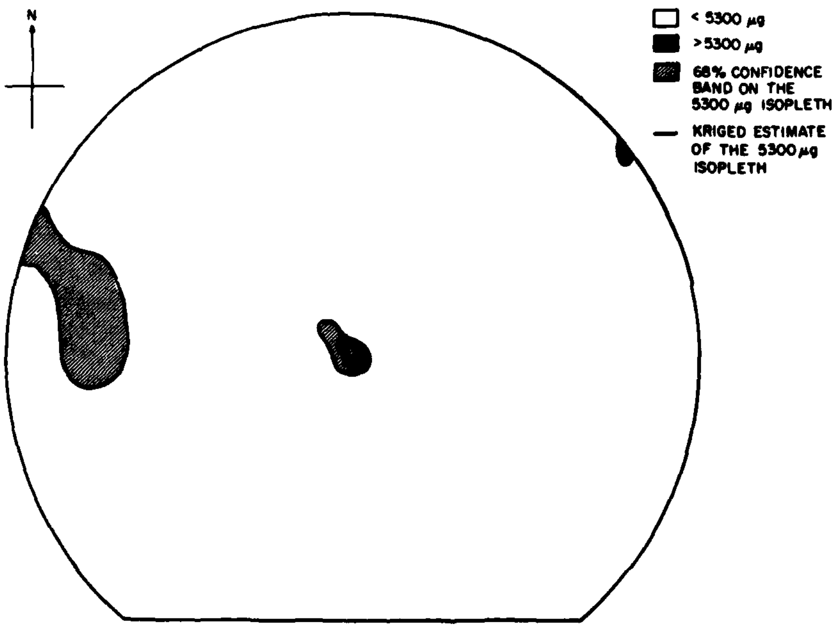

Fig. 11.
Contour map of the 5300-μg isopleth for the kriged surface.

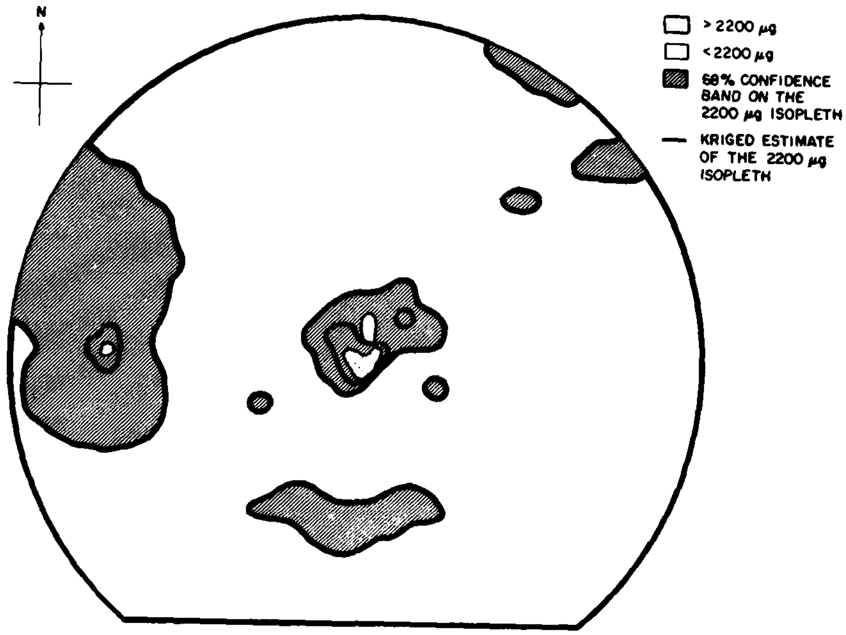

Fig. 12.
Contour map of the 2200-μg isopleth for the kriged surface.

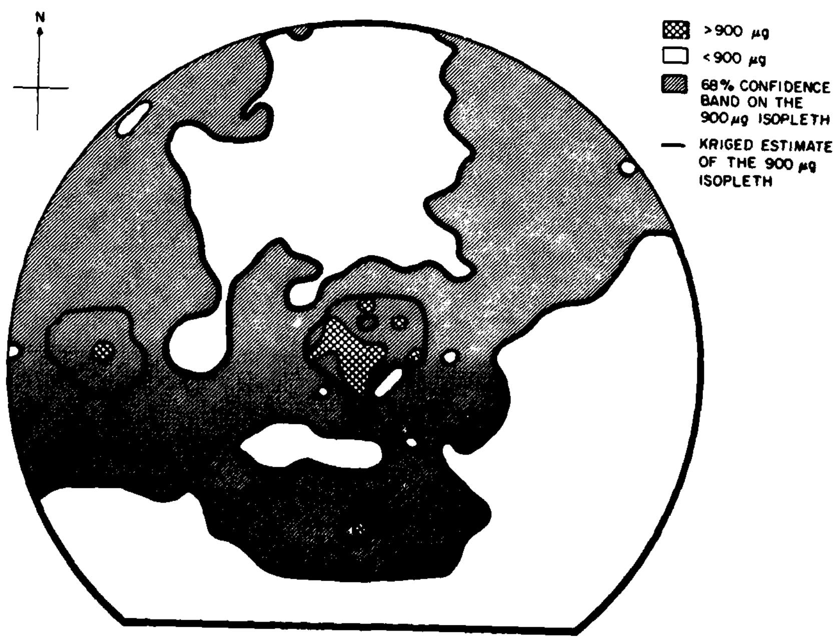

Fig. 13.
Contour map of the 900-μg isopleth for the kriged surface.

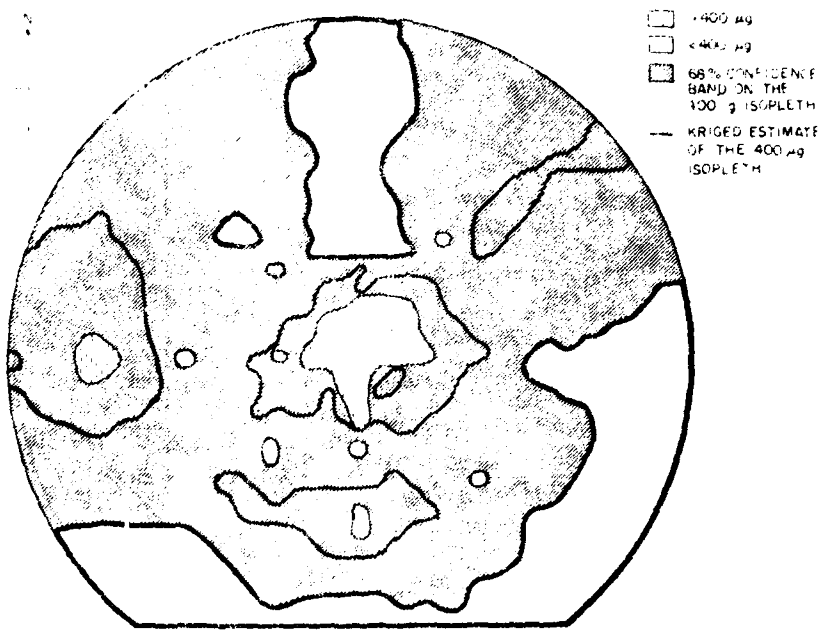

Fig. 14.
Contour map of the 400-μg isopleth for the kriged surface.

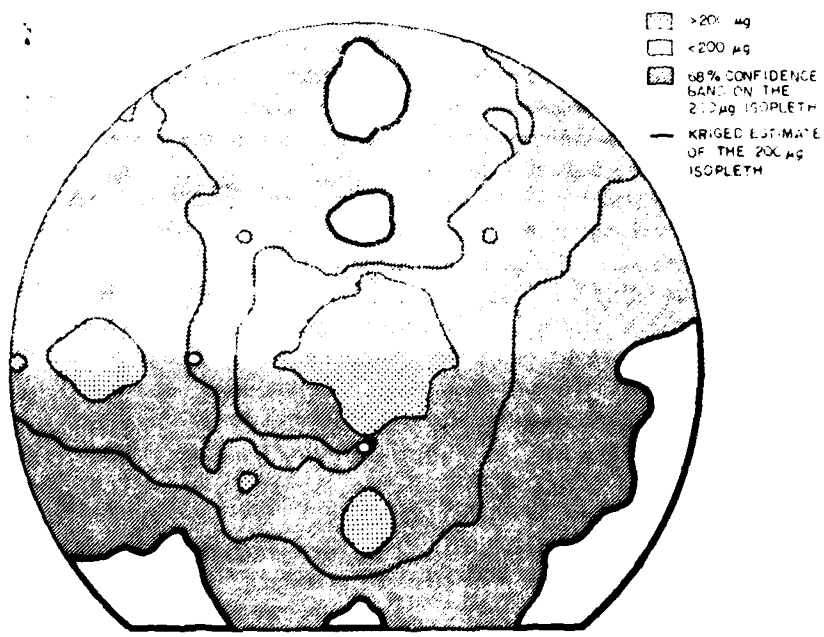

Fig. 15.
Contour map of the 200-μg isopleth for the kriged surface.

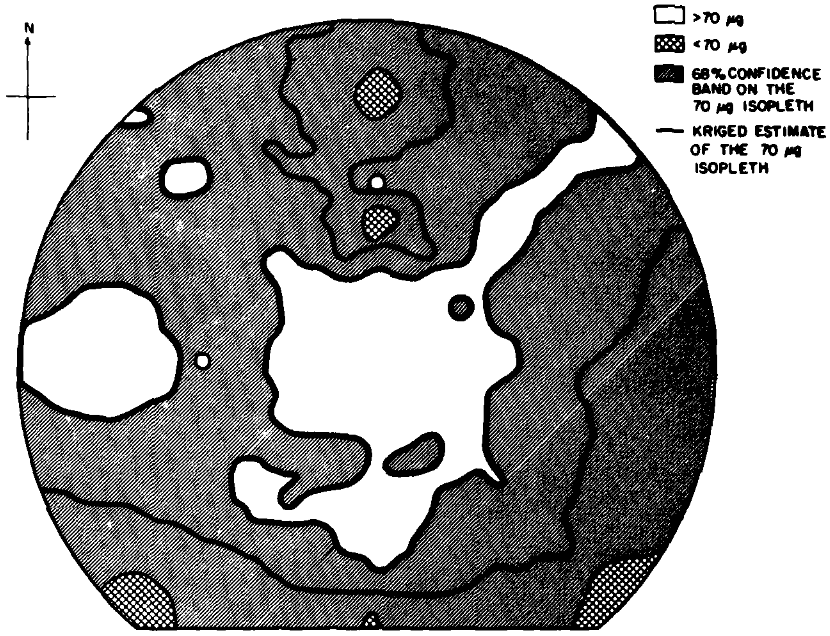

Fig. 16.
Contour map of the 70-μg isopleth for the kriged surface.

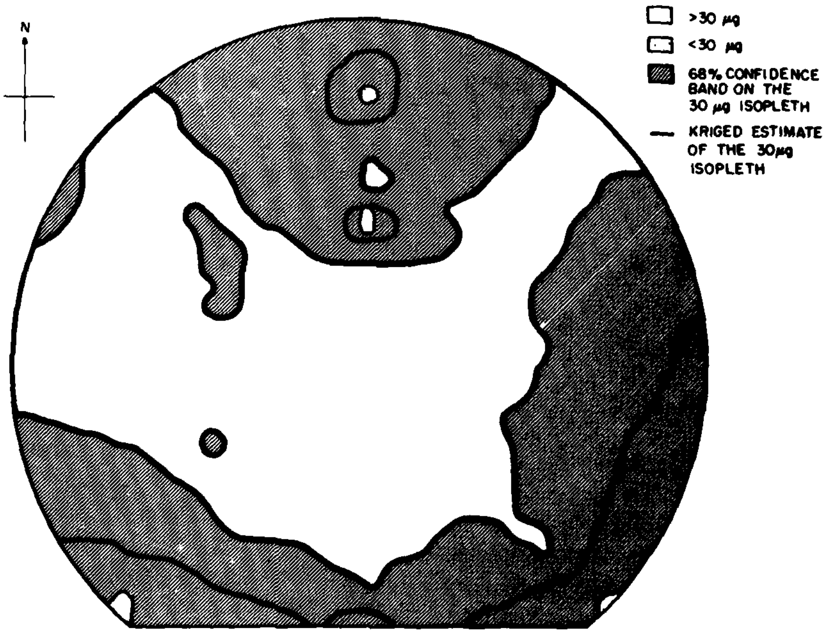

Fig. 17.
Contour map of the 30-μg isopleth for the kriged surface.

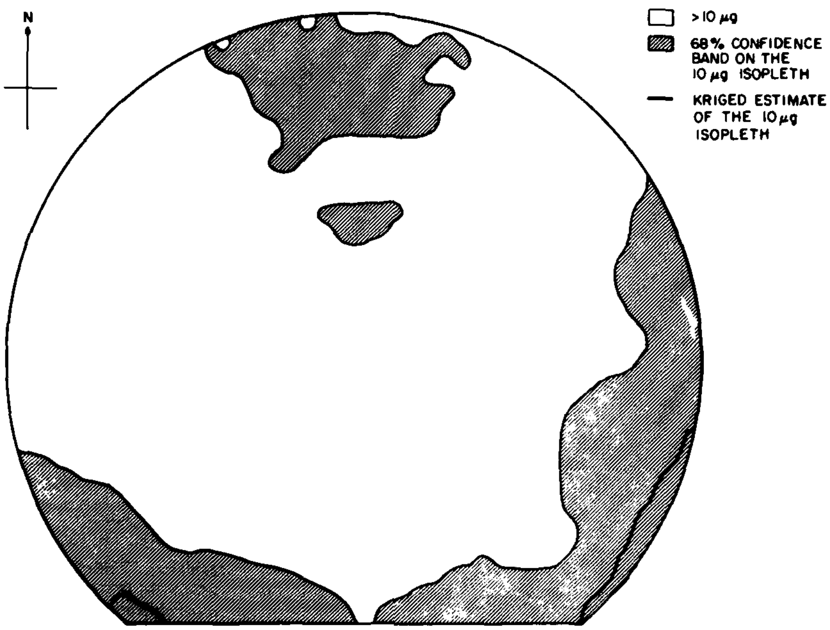

Fig. 18.

Contour map of the 10-μg isopleth for the kriged surface.

Two major factors involved in the large variation in the kriged surface are the apparent discontinuity in the uranium concentrations and the radial sampling pattern used.

Ten pairs of data points were only 0.5 m apart:

Data Points	% Difference
(1100)(157)	601
(417)(105)	297
(482)(94)	413
(3900)(1100)	255
(8600)(7800)	10
(2632)(420)	527
(1900)(896)	112
(1500)(887)	69
(725)(525)	38
(155)(65)	138

The fluorometric technique has a standard deviation of ±10%, yet 9 of the 10 pairs differed by much more than 10%. Sampling methods can also account for some of the variability. In addition, the uranium was originally in canisters that were placed at the detonation point and exploded. The terrain surrounding the detonation point had bunkers to the north and south, and roads were cut through the area. Although small particles of uranium may have smoothly blanketed the area, larger pieces were also thrown about, causing discontinuity in the uranium concentrations.

The radial sampling pattern used to collect the data was designed to give the most information about the area closest to the detonation point. This sampling design would have provided less variable estimates if the detonation point had been smooth (continuous) in the outer areas. Unfortunately, this is not the case at E-F Site. As discussed above, the uranium concentrations at E-F Site appear to be discontinuous. Although there is the expected high variability near the detonation point, the greatest variability occurs in the outer areas, which had greater discontinuity. Because of a high uranium concentration (4900 μg) 150 m west of the detonation point (and because other information was inadequate for analysis), high concentrations (>900 μg) with high variability were estimated for a large area.

Because of our experience at E-F Site, we suggest a modified grid sampling pattern, like that shown in Fig. 19, if a similar site is to be studied. This pattern retains a high sampling density near the detonation point while increasing the sampling density in the

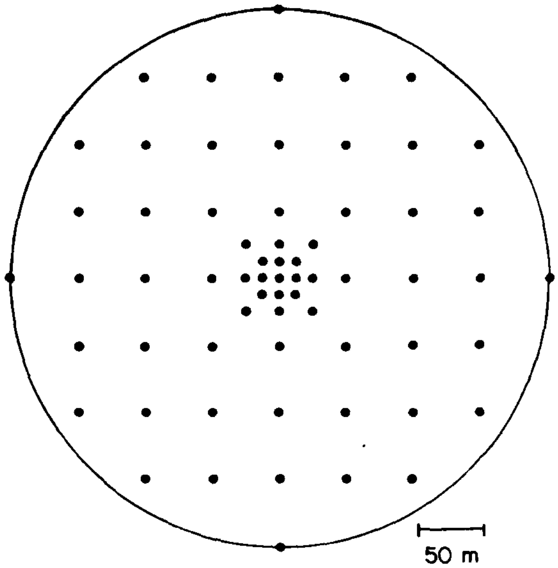

Fig. 19.
Modified grid sampling pattern suggested for sites similar to E-F Site.

outer areas. Also, for the same sampling effort (82 data points), the number of sampling points within 0.5 m of another point should be increased to 17 and spread throughout the area. This would increase kriging's ability to quantify the nugget effect. The increased sampling density in the outer area would also help decrease the effect of any uranium nuggets found in the sampling.

A second technique known as trend analysis[6] was also used to analyze the uranium concentrations in the surface soil at E-F Site. In trend analysis, uranium concentration is assumed to be approximated by a limited sequence of terms, such as a polynomial based on Cartesian coordinates. To apply trend analysis to the E-F Site data, the exponential of a fourth-degree polynomial was fitted to the uranium concentrations C;

$$C_i = \exp\left\{\Sigma\ \Sigma\ \beta_{jk} X_i^{\,j} Y_i^{\,k} + e_i\right\}$$

$$(j = 0, 4,\ k = 0, 4,\ j + k \leq 4) \quad ,$$

where C_i is the uranium concentration at location (X_i, Y_i), with i = 1, ..., n, and β_{jk} is the jkth regression coefficient estimated by minimizing the sum of squared errors

$$\sum_{i=1}^{n} e_i^{\,2} \quad .$$

To reduce the parameter space (number of β's), the leaps and bounds algorithm RLEAP[6] was used to select a subset of the combination X^jY^k. We determined the best fitting model to be (with the i subscript dropped)

$$C_i = \exp(6.995 - 0.4144E{-}2\ Y - 0.3013E{-}3\ Y^2$$
$$- 0.6533E{-}4\ X^2 + 0.3081E{-}6\ XY^2$$
$$+ 0.8870E{-}6\ X^2Y - 0.2661E{-}6\ X^3$$
$$+ 0.6346E{-}8\ Y^4 + 0.4462E{-}8\ X^2Y^2) \quad .$$

A contour plot of this function is shown in Fig. 20.

To estimate average surface concentration, the volume under this surface in the 200-m-radius circle was found by

$$V = \int_{-200}^{+200} \int_{-\sqrt{200^2 - x^2}}^{\sqrt{200^2 - x^2}} C\ dy\ dx$$

V is converted to concentration by dividing by the area of the circle, 4E4 m^2, giving an average concentration of 268 μg/g soil. This estimate exceeds the average concentration estimated by kriging of 159 μg U/g soil (± 1 SE, 117-218). However, comparison of the contour plots in Figs. 5 and 20 for kriging and trend analysis shows that the polynomial was unable to model the decline and then increase in uranium concentration to the west of the (0,0) station, whereas kriging allows for the decline in concentration at station (−100, 0). Thus, much of the dis-

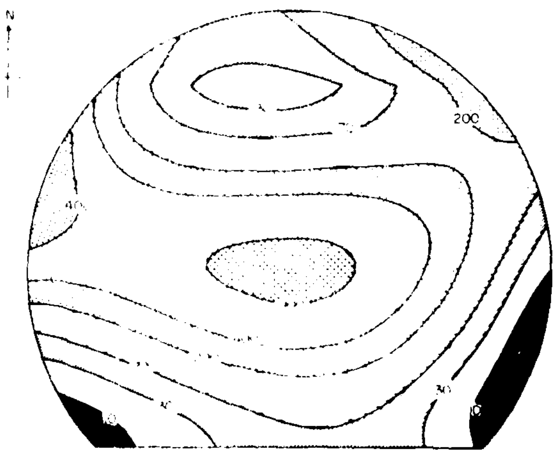

Fig. 20.
Trend analysis contour map of uranium concentrations (μg U/g soil) from E-F Site.

crepancy is explained by comparing contour maps of both fitted surfaces with that developed from empirical data (Fig. 6).

For the variable type of data collected at E-F Site, kriging appears to be the more useful approach to estimating mean concentration. Trend analysis assumes that the true surface being modeled is smoother than is the actual case. The discontinuities in concentration caused by the original distribution of the uranium are not modeled well by a smooth surface.

III. COUNTING EFFICIENCY OF THE PHOSWICH PORTABLE SURVEY INSTRUMENT

One possible drawback of the phoswich field instrument is that its counting efficiency is affected by the ambient air temperature.[7] To establish a calibration curve for the phoswich detector to compensate for variability caused by changes in ambient temperature, soil moisture, and relative humidity, a controlled environment experiment was set up in a Percival Model PT80 growth chamber.

Temperature in the chamber was controlled by placing the chamber's maximum and minimum temperature controls at the same setting. Accuracy of these settings in the chamber was determined using a Weston Bi-metal Thermometer (range 0-50°C), a Weathermeasure Model H-311 Recording Hygrothermograph, and a Lufft-Abbeon Model M2A4B Temperature/Relative Humidity Gauge. The last two instruments also provided relative humidity measurements inside the chamber.

The phoswich was mounted on laboratory stands in the chamber to maintain a fixed geometry. A lab-jack was used to position soil samples under the opening in the phoswich columnator (Fig. 21). Five sample containers measuring 8.6 cm by 9 cm by 5.5 cm deep, which corresponded to the opening in the columnator shielding, were constructed of Lucite.

Soil collected from near the detonation point at E-F Site was dried at 90°C for 48 hours, sifted through a 4000-μ (US#5) standard sieve, and mixed in a twin-shell blender for 1 hour. Four aliquots weighing 572.6, 564.7, 560.7, and 570.6 g, respectively (oven-dry weight), were placed in the sample containers. The fifth container was left empty to obtain background readings for the phoswich. The samples were then placed in the growth chamber at 10°C, allowed to equilibrate to temperature overnight, and counted on the phoswich to establish a dry-weight base-line count. No water, and 50, 100, and 150 mℓ of distilled water were added to the four samples to provide a range of soil moisture. The samples were reweighed, placed in the growth chamber at 10°C, allowed to equilibrate, and recounted.

The temperature in the chamber was increased in 5°C increments from 10-30°C. The chamber, instruments, and samples were allowed to equilibrate overnight after each temperature change. Soil samples were reweighed daily. Because of evaporation at higher temperatures, it was not possible to hold soil

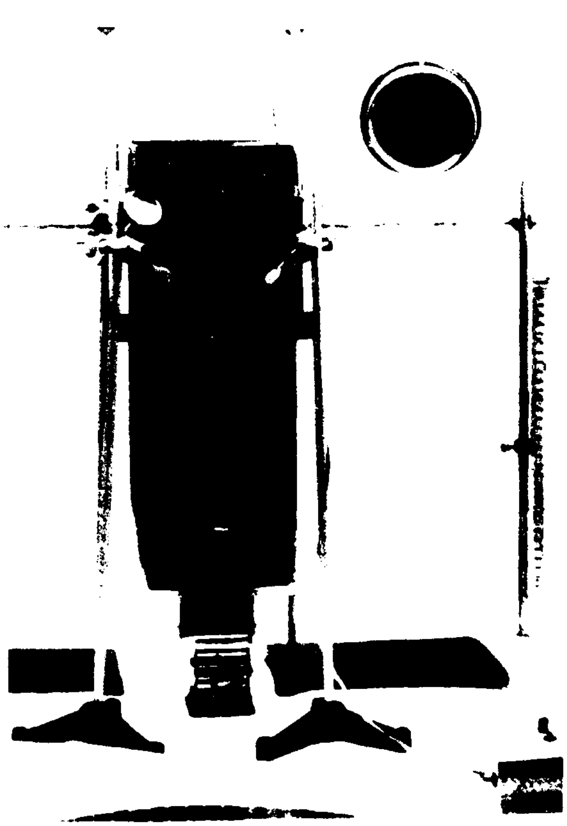

Fig. 21.
Arrangement of the phoswich counter and soil sample in the environmental chamber. The soil sample (A) is positioned on the lab-jack under the phoswich.

moisture constant throughout the experiment. Samples were counted in random sequence to avoid possible bias.

A multiplicative model was fitted to the environmental chamber data because of the effects of temperature, relative humidity, and soil moisture on counting efficiency. Thus, for example, a decrease in temperature caused an increase in the number of counts. The multiplicative model was transformed into an additive model by taking the logarithm of the phoswich counts

$$C_i = \exp(I_j + B_1X_1 + \ldots + B_kX_k + e_i) \quad ,$$

where C_i is the number of counts for case i, e_i is the error term, I_j is the intercept for the jth soil sample (j=1, ...,4), and B_1 to B_k are the regression coefficients for the ℓth covariate ℓ=1,...,k. The covariates considered were temperature, relative humidity, and bulk density of the soil, plus squared and cubic terms for each of these covariates, giving a total of k = 9 covariates. Regression analysis revealed that only temperature was useful in predicting the phoswich count. However, the phoswich counts tended to follow a nonlinear function of temperature with the best fitting regression line involving only linear and square terms of temperature (T).

$$C_i = \exp(\mu + I_i + 0.296\text{E-}1T - 0.130\text{E-}2T^2 + e_i) \quad ,$$

where r^2 = 93%, $F_{(5,93)}$ = 242.8 (P < 0.001), and the standard errors of the linear and quadratic coefficients are 0.450E-2 and 0.120E-3, respectively. The plot of phoswich counts vs temperature is shown in Fig. 22. Note that the different regression lines are due to sample activity, not to soil moisture.

The equation relating phoswich counts to temperature indicates the importance of recording temperature when using the instrument in a quantitative analysis. The effect of temperature is not linear, so changes in temperature at 30°C do not have the same effects as a similar change at 10°C. To standardize phoswich counts to 10°C, the above equation is rearranged to give

$$\begin{aligned}\text{standardized count} &= \exp(\ln(\text{Count}) \\ &\quad - 0.296\text{E-}1T + 0.130\text{E-}2T^2 + 0.166) \\ &= \text{Count} \cdot \exp(-0.296\text{E-}1T + 0.130\text{E-}2T^2 + 0.166) \quad .\end{aligned}$$

IV. PHOSWICH COUNTS COMPARED TO IENA MEASUREMENTS

In February 1979, the phoswich survey instrument was used to resurvey the inner four rings of sampling locations on Test Area C-74L (EAFB). After a 500-s count was completed, a 10- by 10- by 1-cm^3 soil sample was collected for IENA.[6] The physical size of the soil sample corresponded to the opening in the columnator shielding. The samples were ball-milled and a l-g aliquot was taken. Previously, soil samples from Test Area C-74L were sieved to remove the larger chunks of uranium, but to maintain compatibility with the phoswich count, the chunks of uranium in our samples were not removed before the IENA. Net phoswich counts were standardized to 10°C.

Figure 23 is a plot of the results. Although the fitted line y = −122.8 + 0.728x provides a statistically significant fit (P < 0.001, r^2 = 0.84), the data are not satisfactorily fit by a linear function. Also, any inferences from this data set would be suspect because of the clustering of the data near the origin. Most of the locations sampled have a low or zero concentration, but 2 data points with standard phoswich counts greater than 1000 tend to contribute greater weight to the analysis than they should.

These results raise questions about the usefulness of the phoswich as a quantitative instrument to be used for a double-sampling approach to quantitatively measure uranium in the field.[7] Before a large-scale study using this technique is initiated, a laboratory study should be conducted to calibrate the phoswich instrument with soil samples of known uranium concentrations. However, the data indicate that the phoswich is adequate for qualitative surveys above some detection limit.

V. CONCLUSIONS

The statistical technique called kriging provided a much more realistic contour surface for E-F Site uranium concentrations than either a polynomial trend analysis or contouring the original data. The major advantages of kriging are that a measure of the uncertainty of the contoured surface is provided, and that the nonparametric nature of the method allows very irregular surfaces to be fitted.

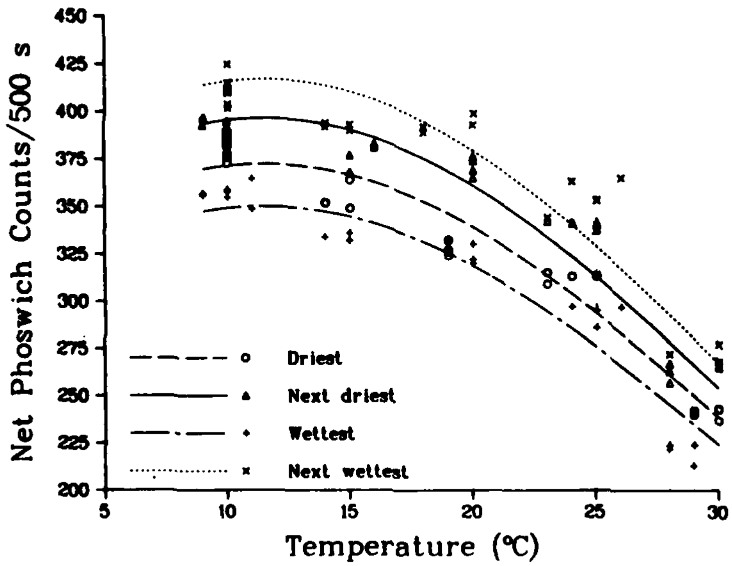

Fig. 22.
Phoswich counts vs temperature for the environmental chamber data.

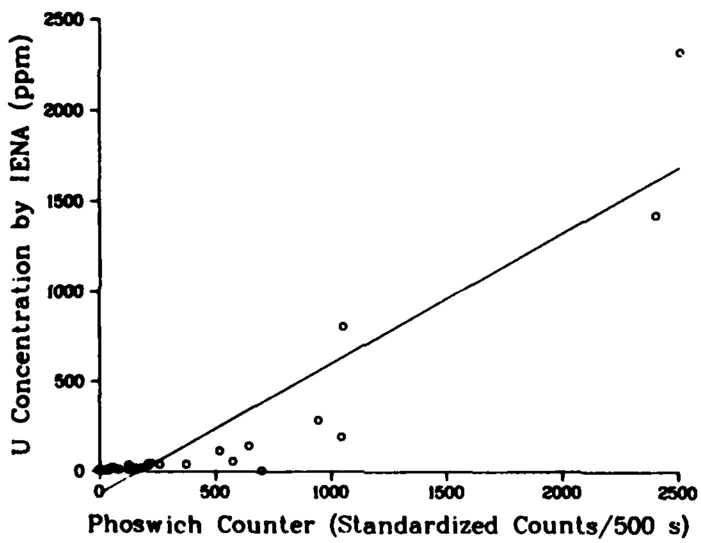

Fig. 23.
Phoswich counts vs temperature for the environmental chamber data.

A calibration curve was developed to correct the phoswich survey instrument for temperatures from 10-30°C. Counting efficiency is maximum at approximately 10°C and declines significantly at higher temperatures. Before the phoswich instrument is used extensively for quantitative surveys of uranium, a laboratory study should be conducted to calibrate the instrument with soil samples of known uranium concentrations.

ACKNOWLEDGMENTS

We appreciate the assistance of J. L. Martinez, E. S. Gladney, and D. R. Perrin in preparation and chemical analysis of soil samples, and R. O. Gilbert, T. E. Hakonson, W. R. Hanson, and A. J. Ahlquist in reviewing a preliminary draft of this report.

REFERENCES

1. W. C. Hanson and F. R. Miera, Jr., "Long-Term Ecological Effects of Exposure to Uranium," Los Alamos Scientific Laboratory report LA-6269 (July 1976).

2. W. C. Hanson and F. R. Miera, Jr., "Continued Studies of Long-Term Ecological Effects of Exposure to Uranium," Los Alamos Scientific Laboratory report LA-6742 (AFATL-TR-77-35) (June 1977).

3. W. C. Hanson and F. R. Miera, Jr., "Further Studies of Long-Term Ecological Effects of Exposure to Uranium," Los Alamos Scientific Laboratory report LA-7162 (AFATL-TR-78-8) (July 1978).

4. P. G. Doctor, "An Evaluation of Kriging Techniques for High Level Radioactive Waste Repository Site Characterization," Battelle Pacific Northwest Laboratory report PNL-2903/UC-70 (January 1979).

5. F. P. Agterberg, *Geomathematics* (Elsevier, New York, 1974), pp. 279-309.

6. International Mathematical and Statistical Libraries, "The IMSL Library," IMSL LIB-0007 (January 1979).

7. G. C. White, E. S. Gladney, K. V. Bostick, and W. C. Hanson, "Studies of Long-Term Ecological Effects of Exposure to Uranium IV," Los Alamos Scientific Laboratory report LA-7750 (AFATL-TR-79-9) (May 1979).

8. E. S. Gladney, J. W. Owens, and J. W. Starner, "Simultaneous Determination of Uranium and Thorium in Ores by Instrumental Epithermal Neutron Activation Analysis," Anal. Chim. Acta 104, 121-127(1979).

DISTRIBUTION

Accessions Division DTIC (2)
Cameron Station
Alexandria, VA 22314

AUL/LSE 71-249
Maxwell AFB, AL 36112

ASD/ENFEA
Wright-Patterson AFB, OH 45433

AFATL/DLODL (9)

AFATL/DL

Hq USAF/SAMI
Bolling AFB, Washington, DC 20332

OOALC/MMWMP
Hill AFB, UT 84406

AFIS/INT
Washington, DC 20330

ASD/ENESH S. Johns
Wright-Patterson AFB, OH 45433

Hq TAC/DRA
Langley AFB, VA 23665

HQ USAFE/DOQ
APO New York 09012

Hq PACAF/DOOFQ (3)
Hickam AFB, HI 96853

TAC/INAT
Langley AFB, VA 23665

ASD/XRP
Wright-Patterson AFB, OH 45433

Director
US Army TRADOC Systems Analysis Activity
ATTN: ATAA-SL (Tech Lib)
White Sands Missile Range, NM 88002

COMIPAC/I-232
Box 38
Camp H. M. Smith, HI 96861

DDR&E (Tech Lib)
Rm 3E1014
Pentagon
Washington, DC 20301

USAFA/DFCBS
USAF Academy, CO 84406

AFSC/SDW
Andrews AFB
Washington, DC 20334

HQ USAF/RDP
Washington, DC 20330

DDR&E (Env & Life Sciences)
Rm 3E1014
Pentagon
Washington, DC 20301

Chemical Systems Lab
DRDAR-CLJ-L (Tech Lib)
Aberdeen Prov Gd, MD 21010

USAF (Env Health Lab)
Kelly AFB, TX 78241

AMD/RD
Brooks AFB, TX 78235

AMRL/THT (Dr. Back)
Wright-Patterson AFB, OH 45433

AFLC/DS
Hill AFB, UT 84406

US Army Natick Lab
Natick, MA 07162

AFATL/DLV (30)
Eglin AFB, FL 32542

Deseret Test Center/
Tech Lib, Dugway Prov Gd
Dugway, UT 84022

NWC/Code 3943 (Mr. Claunch)
China Lake, CA 93555

Commander, ARRADCOM
ATTN: DRDAR-SCM-P
(Dr. Bloore)
Dover, NJ 07801

Battelle Pacific Northwest
Lab (ATTN: Dr. Wayne Hanson)
Richland, WA 99352

1035 TCHOG/TRE
(Dr. Collins)
Patrick AFB, FL 32925

Battelle Pacific Northwest Lab
(ATTN: R. L. Gilchrist)
Richland, WA 99352

Printed in the United States of America. Available from
National Technical Information Service
US Department of Commerce
5285 Port Royal Road
Springfield, VA 22161

Microfiche $3.00

001-025	4.00	126-150	7.25	251-275	10.75	376-400	13.00	501-525	15.25
026-050	4.50	151-175	8.00	276-300	11.00	401-425	13.25	526-550	15.50
051-075	5.25	176-200	9.00	301-325	11.75	426-450	14.00	551-575	16.25
076-100	6.00	201-225	9.25	326-350	12.00	451-475	14.50	576-600	16.50
101-125	6.50	226-250	9.50	351-375	12.50	476-500	15.00	601-up	

Note: Add $2.50 for each additional 100-page increment from 601 pages up.